

MARIAN ŻENKIEWICZ<sup>1)\*</sup>, PIOTR RYTLEWSKI<sup>1)</sup>, ADAM TRACZ<sup>2)</sup>,  
WALDEMAR MRÓZ<sup>3)</sup>, JÓZEF RICHERT<sup>4)</sup>

## Effects of laser radiation on some properties of the surface layer of polycarbonate

**Summary** — Influence of excimer laser radiation (193 nm) on the oxidation degree, surface geometrical structure, wettability, and surface free energy of the surface layer of polycarbonate was studied. The oxidation degree was monitored by the X-ray photoelectron spectroscopy (XPS) while changes in the surface geometrical structure by the atomic force microscopy (AFM). The contact angles of test liquids (water and diiodomethane) were measured with use of a goniometer, the surface free energy was calculated by the Owens-Wendt method. It was found that the nature of the physicochemical changes occurring in the polycarbonate surface layer upon laser irradiation depends mostly on the wavelength of the laser radiation, unit energy of a laser pulse, and number of the laser pulses. It was found that the ArF excimer laser is an effective tool for modification of the polycarbonate surface layer, unlike the XeCl laser the radiation energy of which is too low.

**Key words:** polycarbonate, surface layer, laser modification, XPS, AFM, contact angle, surface free energy.

### WPLYW PROMIENIOWANIA LASEROWEGO NA NIEKTÓRE WŁAŚCIWOŚCI WARSTWY WIERZCHNIEJ POLIWĘGLANU

**Streszczenie** — Zbadano wpływ promieniowania lasera ekscymerowego ( $\lambda=193$  nm) na stopień utlenienia warstwy wierzchniej (SL) (wartości stosunku O/C) (rys. 1—3), strukturę geometryczną powierzchni (rys. 4—9) oraz zwilżalność i swobodną energię powierzchniową poliwęglanu (PC) (rys. 10—15). Stopień utlenienia oceniano metodą spektroskopii fotoelektronowej (XPS) a strukturę geometryczną powierzchni — metodą mikroskopii sił atomowych (AFM). Wyniki pomiarów (za pomocą goniometru) kąta zwilżania PC wodą i diiodometanem stanowiły podstawę obliczeń swobodnej energii powierzchniowej, przeprowadzonych metodą Owensa-Wendta. Wykazano, że zmiany fizykochemicznych cech warstwy wierzchniej PC zachodzące pod wpływem promieniowania laserowego zależą od długości fali tego promieniowania, jednostkowej energii impulsu laserowego oraz od liczby impulsów. Stwierdzono, że laser ekscymerowy ArF jest skutecznym narzędziem modyfikowania warstwy wierzchniej poliwęglanu, w przeciwieństwie do używanego w serii prób wstępnych lasera XeCl ( $\lambda = 308$  nm), który ma za małą energię promieniowania do tych zastosowań.

**Słowa kluczowe:** poliwęglan, warstwa wierzchnia, modyfikowanie laserowe, XPS, AFM, kąt zwilżania, swobodna energia powierzchniowa.

### PECULIARITY OF THE PROCESS OF POLYMER SURFACE LAYER MODIFICATION WITH LASER

Properties of the surface layer (SL) of polymeric materials strongly affect functional quality of many modern products. Most of these materials are insufficiently reactive, extremely hydrophobic, and exhibit distinctly low surface free energy (SFE), what negatively influences

their wettability by paints, lacquers, glues, and decorative agents. In order to reduce these drawbacks, *i.e.*, to enhance the material adhesive properties, various methods have been applied to modify the SL. They consists mainly in initiation of chemical reactions that cause the formation of polar functional groups within the SL and in changes of the surface geometrical structure of the material to be modified. As a result, the processes of oxidation, crosslinking and/or degradation, as well as disintegration of polymer macromolecules occur [1—2].

The laser modification of the SL of polymeric material makes possible to change precisely various properties of this layer, such as wettability and SFE (occurring due to formation of polar functional groups mostly as a result of the oxidation process), degree of crosslinking, and type of the surface geometrical structure, including surface roughness. At the same time, this treatment does not

<sup>1)</sup> Kazimierz Wielki University, Department of Materials Engineering, ul. Chodkiewicza 30, 85-064 Bydgoszcz, Poland.

<sup>2)</sup> Centre of Molecular and Macromolecular Studies, Polish Academy of Sciences, ul. Sienkiewicza 112, 90-363 Łódź, Poland.

<sup>3)</sup> Military University of Technology, ul. Kaliskiego 2, 00-908 Warszawa 49, Poland.

<sup>4)</sup> Institute for Engineering of Polymer Materials and Dyes, ul. M. Skłodowskiej-Curie 55, 87-100 Toruń, Poland.

<sup>\*)</sup> Corresponding author, e-mail: marzenk@ukw.edu.pl

change the properties of the bulk of the material, *i.e.* of the material part below the layer being modified. The laser modification technique is simple, easily controllable, and environmentally friendly. However, the physicochemical phenomena and application issues concerning this method are continually a subject of intensive studies [3–6].

Selection of a suitable laser intended for modification of a polymer SL is not easy. One has to consider optical and thermal properties of the material to be modified, wavelength and intensity of the laser radiation, mode of operation and consumption of a laser active medium, and investment costs. The effects of the laser treatment depend also on the kind of the surface of the polymer being modified: materials of a rough surface usually absorb more energy of the laser radiation than the smooth ones [7].

Furthermore, the results of the SL modification are largely relative to the absorption coefficient of the irradiated material, being a function of the laser radiation wavelength. The latter is associated with the photon energy and, thus, it constitutes one of the most important factors of the laser modification process. The high-power CO<sub>2</sub> lasers, operating in the region of long waves ( $\lambda = 9\text{--}11\ \mu\text{m}$ ), *i.e.* of low-energy photons, cause ablation of polymer materials rather than breaking of chemical bonds of macromolecules. On the contrary, the excimer lasers, operating in the region of the UV radiation that is strongly absorbed in most of polymers, initiate photochemical reactions without causing any thermal damages. Therefore, the excimer lasers may be used to modify the SL of polymers in order to improve adhesion properties of the latter. As a result, a ten-fold increase in the strength of the adhesive-bonded joints can be achieved [6, 7].

Breaking of chemical bonds of a main chain or of side chains of polymer macromolecules, occurring upon the laser radiation, leads to formation of radicals that react with oxygen. Before the irradiation is initiated, the polymeric material is in the state of thermodynamic equilibrium with an air and, in general, its SL contains more oxygen compared to the amount resulting from the elemental composition of the polymer. Oxidation of this layer causes the formation of polar functional groups in it, which enhances its wettability and, thus, improves its adhesion properties [10, 11]. Photocrosslinking occurring in the polymer SL is another effect of the laser irradiation [12, 13].

Upon the laser radiation, the removal of macromolecule fragments from the polymer SL, called laser ablation, can appear as well. This phenomenon commonly occurs during an erosion-related treatment of various polymeric materials. Changes in the surface geometrical structure of polymeric materials are additional effects of the laser ablation [14, 15].

The advantages of lasers in the processes of the polymer SL modification, especially ease and rate of these

processes, limitation of changes in properties of the materials being modified to a depth not greater than 10  $\mu\text{m}$ , possibility to form precise surface areas of complex shapes, and lack of environmental pollution, create real perspectives of a rapid development of application of this technique in the industry, *e.g.*, in microelectronics. However, it has to be taken into account that, during the process of the laser modification of the polymer SL, degradation and/or destruction [16] as well as crosslinking [17] of the polymer can occur, which not always are beneficial to the modification purpose.

The aim of this work was to investigate the influence of conditions of the laser irradiation on the properties of the surface layer of polycarbonate (PC), mainly in the region of laser pulse energies below the PC ablation threshold. For this energy region, the photochemical processes that improve the adhesion properties of the polymer modified this way dominate. There were studied by us the extent of oxidation and elemental composition of the SL, surface geometrical structure, as well as wettability and surface free energy of the PC samples irradiated in different ways with an excimer laser.

## EXPERIMENTAL

At the beginning, preliminary measurements were performed, the results of which were used to select both the suitable PC from a group of thermoplastics and the appropriate laser type (ArF), which were to be applied in further experiments. Use of the XeCl laser of  $\lambda = 308\ \text{nm}$  was omitted because modification effects were insufficient due to too low energy of photons. Preliminary conditions of preparation and irradiation of the studied samples were also determined.

### Materials

— Polycarbonate (PC) designated as Lexan 143 R (GE Plastics, USA) was used to perform the investigation. Its melt flow rate (MFR) was 10.5 g/10 min and density ( $d$ ), 1.2 g/cm<sup>3</sup>.

— Redistilled water (Maggie Co, Poland) and diiodomethane (Sigma-Aldrich GmbH, Germany) were used as polar and disperse liquids, respectively, in the contact angle measurements.

### Instruments

The following instruments were applied in the investigations:

— Plus 35/75 UNILOG B2 laboratory injection molding press (Battenfeld GmbH, Germany) with a screw of the 22 mm diameter, 38 cm<sup>3</sup> injection volume, and 200 MPa nominal injection pressure, was used to form the samples studied.

— ArF LPX 300 excimer laser (Lambda Physik, Germany), with a wavelength of 193 nm (photon energy of

6.4 eV), pulse energy of 100–400 mJ, pulse duration of 15–20 ns, and pulse repetition rate of up to 50 kHz, was used to irradiate the samples.

— Escalab 210 photoelectron spectrometer (VG Scientific, UK), equipped with an  $AlK_{\alpha}$  X-ray source (photon energy of 1486.6 eV), was applied to determine the elemental composition of the sample SL.

— Nanoscope IIIa atomic force microscope (Veeco Metrology & Instruments Inc., USA), with a minimum resolution of 0.1 nm laterally and 0.01 nm vertically, dedicated to imaging surface geometrical structure and its variation upon irradiation of the samples.

— DSA 100 goniometer (Krüss GmbH, Germany), equipped with an automated dosing system for test liquids and with CCD camera of a maximum framerate of 100 images/s, designed to measure the contact angles.

### Samples preparation and irradiation

Before the injection molding was carried out, the granulated PC was dried at 120 °C for 4 h. Based on the initial experiments, temperatures of zones I and II and of head of the injection molding press were set to 300, 310, and 310 °C, respectively, the injection pressure to 15 MPa, and duration of the molding cycle to 25 s. The mold was designed to produce square plates of PC (60×60×1 mm) from which individual samples (20×10×1 mm) were cut out. The samples were then irradiated in an air.

The exact value of the pulse energy was measured at the laser output using a special measuring instrument. The energy of a laser beam is strongly absorbed by an air, which makes possible to control the energy of the incident beam by varying the distance between the sample and the laser. The required values of this distance were calculated according to Hitchcock *et al.* [18]. This way, there were applied two values (6 and 25 mJ/cm<sup>2</sup>) of the unit energy ( $E_u$ ) of a laser pulse falling on the PC surface being modified. The first value was equal to 1/3 of that relating to the ablation threshold of PC (18 mJ/cm<sup>2</sup>) [19] and the other one was larger by 40 % than the threshold value. The differences between the  $E_u$  values and the ablation threshold were large enough to secure as much as possible a homogeneous nature of changes occurring within the SL. For the smaller value of  $E_u$ , mostly the photochemical processes take place, while in the other case the ablation ones. The calculated laser-to-sample distances were 400 and 70 cm, respectively.

According to the preliminary tests, it was decided to apply five levels of the irradiation energy, relating to different numbers of the laser pulses. Thus, ten samples varying in the value of the absorbed laser energy were prepared. The samples irradiated with the pulses of the energy  $E_u = 6 \text{ mJ/cm}^2$  were denoted as AX, where X = 0, 1, 2, 3, 4, and 5, relating to the pulse numbers of 0 (the non-irradiated sample), 10, 100, 500, 1000, and 2000 pulses. The samples irradiated with the pulses of  $E_u = 25 \text{ mJ/cm}^2$  were designated as BX, where X = 0, 1, 2, 3, 4,

and 5, relating to the pulse numbers of 0 (the non-irradiated sample), 1, 20, 70, 300, and 1500 pulses.

### Measurements

#### X-ray photoelectron spectroscopy (XPS)

In order to limit the degradation of PC, the XPS measurements were carried out using a radiation beam power lowered to 200 W, the nominal power being 300 W. During the measurements, the pressure in the ultra-high vacuum chamber of the XPS system increased from  $6 \cdot 10^{-7}$  to  $8 \cdot 10^{-6}$  Pa due to the desorption of polymer fragments and gaseous substances from the samples studied. The photoelectron take-off angle was 90°, which corresponded to the mean thickness of the examined layer of 4 nm. The overview spectra were recorded within the bond energy ( $E_B$ ) region of 0–1350 eV. The bond energy regions for the detailed spectra were selected with respect to the examined individual chemical elements. The measurement steps for the overview, detailed O<sub>1S</sub>, and detailed C<sub>1S</sub> spectra were 0.4, 0.1, and 0.05 eV, respectively.

Individual peaks as components of the O<sub>1S</sub> and C<sub>1S</sub> bands were fitted according to the data published elsewhere [20]. During analyses of the spectra, the principle of the unity of the nature of physical and chemical phenomena relating to all the studied samples was assumed. This implicates that individual carbon atom species exhibit the same electron structure and chemical surroundings. That assumption was used as a basis to calculate the XPS envelope curves, corresponding to individual functional groups in different samples of the same or similar shape,  $E_B$  value, and band halfwidth but varying more or less in intensity [21, 22]. The accuracy of the quantitative analysis referring to the extent of the SL oxidation depends on the quality of the spectrometer parts as well as on the sample physicochemical properties. Differences between the calculated and real values do not exceed several percent of the real values [21] and, thus, do not essentially influence the presented results.

#### Atomic force microscopy (AFM)

The AFM images were taken by both the contact mode (CM) and the tapping mode (TM). In the contact mode, a V-shape cantilever made of Si<sub>3</sub>N<sub>4</sub> and provided with a tip of the curvature radius equal 50 nm (Parc Instruments, Germany) was used while in the tapping mode, a square cantilever made of Si and equipped with a tip of the curvature radius equal 15 nm (NanoProbe, Germany) was applied. All the measurements were carried out in an air with the scan repetition rate of 3 Hz (CM) and 1 Hz (TM). Resolution of the recorded images was 512 × 512 lines. Preliminary examination of the sample surface was made using the CCD camera coupled with an optical system for magnifying the images that were then recorded in the computer memory and displayed on the monitor screen.

### Wettability and SFE determination

During the contact angle measurements the volumes of water (polar liquid) or diiodomethane (disperse liquid) droplets resting on a sample surface were constantly increased and, at the same time, the dynamic contact angle values were measured. The liquid feed rate was set to 5  $\mu\text{L}/\text{min}$  and the droplet volume growth was monitored in the range of 3–9  $\mu\text{L}$ . The profile of the droplet was analyzed while taking into account a fragment including the contact of three phases: the sample studied, test liquid, and air. Such a method let obtain precise and repeatable results. One hundred measurements of the contact angle were carried out for each sample and then mean arithmetic values, standard deviations, and confidence intervals were calculated. The standard deviations from the mean values of the contact angles of water and diiodomethane were 0.3–1.5° and 1.1–2.6°, respectively.

The values of surface free energy of the studied samples were determined by the Owens–Wendt method, being commonly used in the studies of polymeric materials [1, 2]. Possible errors of the obtained SFE values might result from the inaccuracies of both the contact angle measurements and the assumed SFE values for the test liquids. Considering the conditions of the measurements and results of the statistical analysis of these errors, it was estimated that the latter did not exceed 0.5  $\text{mJ}/\text{m}^2$ .

## RESULTS AND DISCUSSION

### Oxidation of the surface layer

Examination of oxidation of the PC surface layer was carried out by XPS method. The  $\text{O}_{1\text{S}}$  and  $\text{C}_{1\text{S}}$  peaks present in the overview spectra were analyzed qualitatively and quantitatively. Such spectra of non-irradiated PC (sample A0, Fig. 1a) and of PC irradiated with 2000 laser pulses (sample A5, Fig. 1b) reveal that the contribution of oxygen atoms in the SL of sample A5 is larger than that in SL of sample A0. This finding is confirmed by a more intense  $\text{O}_{\text{KLL}}$  peak for sample A5 as compared to that for A0 one. This peak is generated by Auger photoelectrons originating from the outermost (valence) shells of the oxygen atoms.

The qualitative analysis of the functional groups present in SL was made using the detailed spectra including  $\text{C}_{1\text{S}}$  and  $\text{O}_{1\text{S}}$  bands for samples A0 and A5 (Figs. 2a–d). The spectra of this kind for samples A1–A4 are similar in shape just differing in the band intensity. Upon the laser radiation, new polar functional groups arise within the SL in addition to the existing ones, like  $\text{O}=\text{COC}=\text{O}$ ,  $\text{COOH}$ ,  $\text{C}(\text{O})\text{C}$ , and  $\text{C}=\text{O}$ . The mechanism of formation of these groups is typical for photodegradation processes. It consists in the reaction of the atmospheric air with the radicals generated by breaking of the C–H and/or C–C bonds. As a result, there are formed, e.g., cyclic

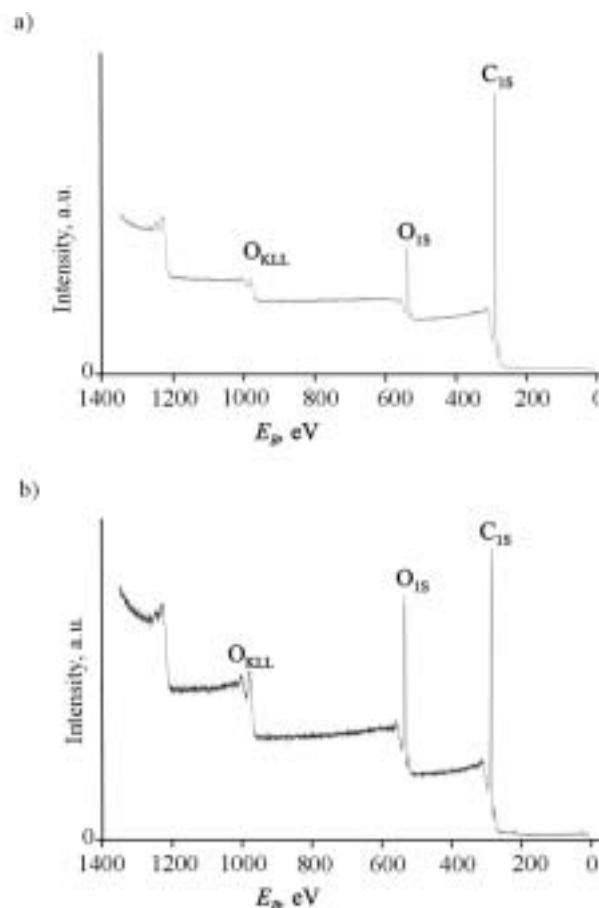


Fig. 1. XPS overview spectra of samples A0 (a) and A5 (b)

groups including connections of one oxygen atom with two carbon atoms. The formation of carbonyl (ketone and/or aldehyde) groups may be associated with breaking of the ether bonds (C–O–C) because the ether groups strongly absorb the laser radiation.

The results of the quantitative analysis of oxidation of SL of all PC samples irradiated at  $E_{\text{ul}} = 6 \text{ mJ}/\text{cm}^2$  with various numbers of the laser pulses are shown in Fig. 3. The extent of oxidation (O/C) is expressed (in %) as the ratio of oxygen and carbon atoms present in the examined SL. Clearly, the value of O/C increases with the rising number of the pulses, the increase being rapid in the region of up to 500 pulses. Under the applied experimental conditions, the O/C value increases almost twice as much if the samples A0 and A5 are considered. This increase is caused by free radicals formed due to the laser irradiation, and reacting with oxygen. According to the theories of photochemical processes occurring in polymers upon the laser radiation, the percentage increment of the amount of products induced by a photochemical reaction varies exponentially with the laser radiation energy [23]. Therefore, the results shown in Fig. 3 have been fitted with a curve described with a function

$$F = a(1 - b \cdot e^{-\beta N}) \quad (1)$$

where:  $a$  — maximum extent of oxidation under the applied conditions of the irradiation ( $a = 25\%$ ),  $b$  — ratio of the extent

of oxidation of sample A0 and  $a$ ,  $N$  — number of the laser pulses,  $\beta$  — parameter proportional to the product of  $E_u$  and the absorption coefficient ( $\beta = 0.004$ ).

A higher O/C value is required for the superior adhesion properties of SL. Introduction of oxygen into PC structure leads to formation of dipole moments in PC macromolecules and, thus, to higher polarity of SL. The dipole moments arise due to large differences among the electronegativities of carbon or hydrogen atoms and that of oxygen ones. Because of these differences, the density of electrons participating in the bonds O-C or O-H is

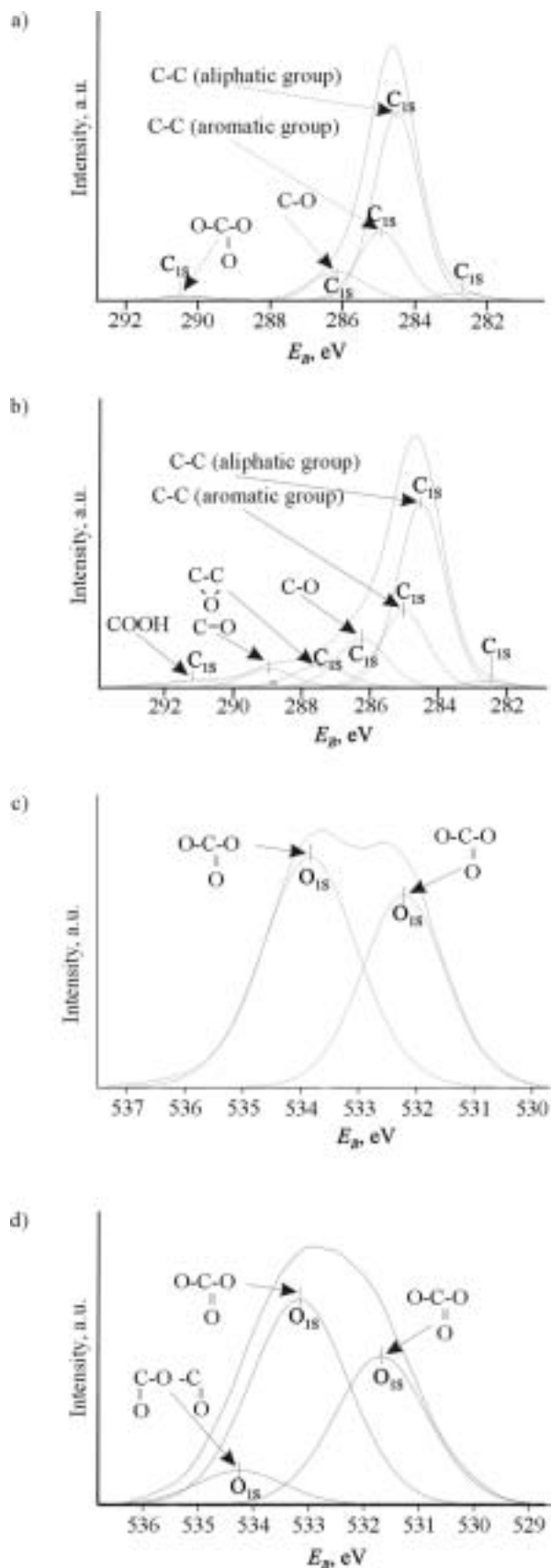


Fig. 2. XPS detailed spectra:  $C_{1s}$  of sample A0 (a),  $C_{1s}$  of sample A5 (b),  $O_{1s}$  of sample A0 (c), and  $O_{1s}$  of sample A5 (d)

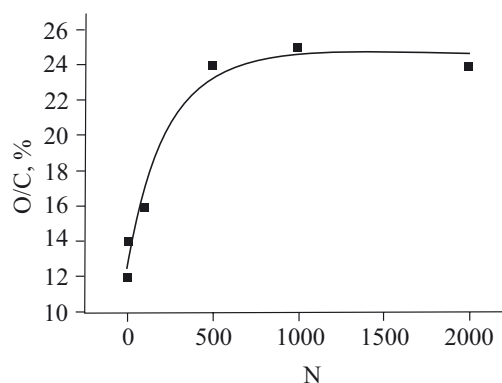


Fig. 3. Extent of oxidation (O/C) of PC surface layer versus the number ( $N$ ) of laser pulses for samples AX. The solid curve was obtained by fitting the data with the equation  $F = a(1 - b \cdot e^{-\beta N})$  (see text)

higher in the surrounding of oxygen atoms than that in the vicinity of carbon or hydrogen atoms. As a result of non-symmetrical distribution of the electric charges, the functional groups including O and C atoms or O and H atoms are of a polar nature.

In SL of samples A0—A4, there were detected trace amounts of silicon (0.3—0.7 %) and in SL of sample A0, also trace amounts of nitrogen (0.2 %) were found. These elements originate probably from anti-adhesion agents used to cover the inside surface of an injection mold.

### Changes in the surface geometrical structure

Upon the laser irradiation, the surface geometrical structure of polycarbonate varies significantly from the initial one. Figures 4a—c show the AFM images of surfaces of samples A0, A3, and A5, recorded in the contact mode in which the overall force is repulsive. Some scratches of sharp contours and definite direction are seen on the surface of sample A0 (Fig. 4a). They reflect the surface geometrical structure of the injection mold inner surface. The laser irradiation causes the contours to diffuse (Figs. 4b, c) and, thus, the surface geometrical structure of PC changes.

In Figures 5a-c there are presented the AFM images of surfaces of samples A0, A3, and A5, recorded at two

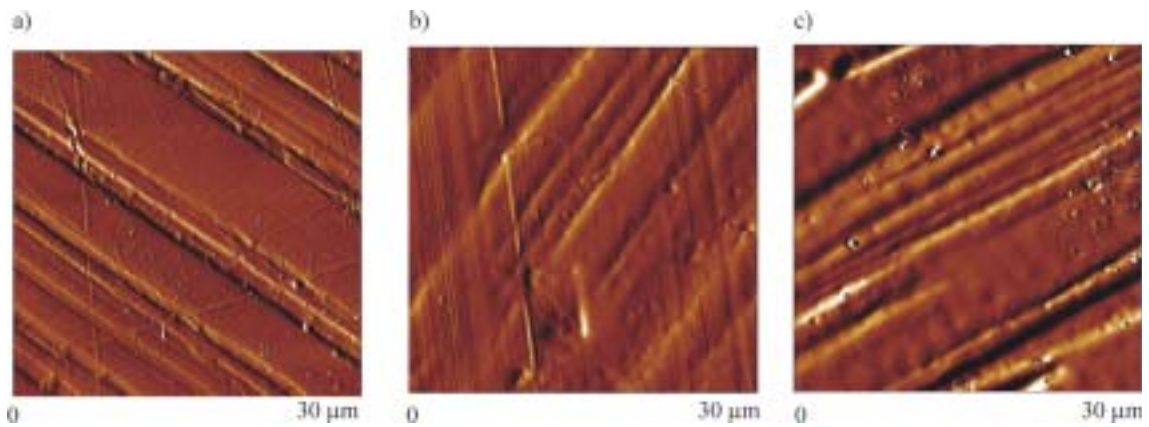


Fig. 4. AFM images of samples A0 (a), A3 (b), and A5 (c), recorded using the contact mode

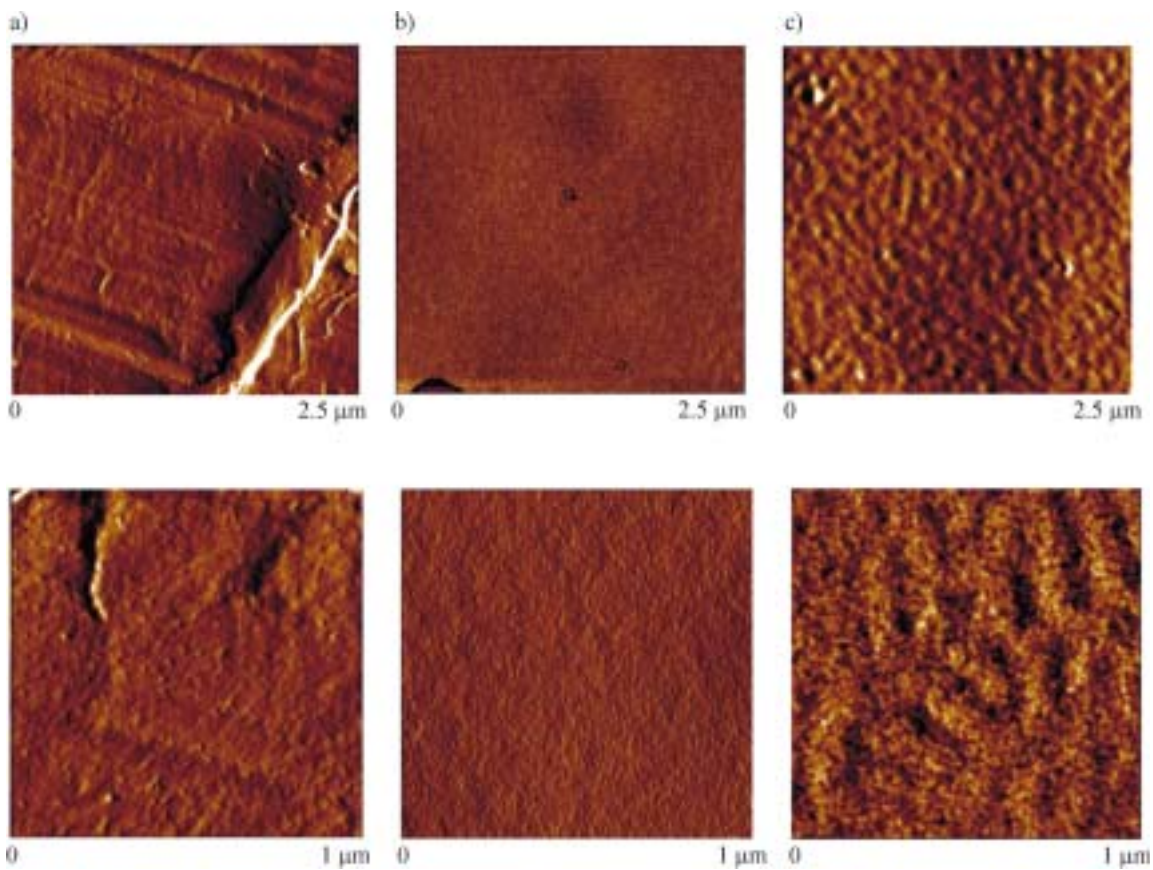


Fig. 5. AFM images of samples A0 (a), A3 (b), and A5 (c), recorded using the tapping mode method at two different magnifications

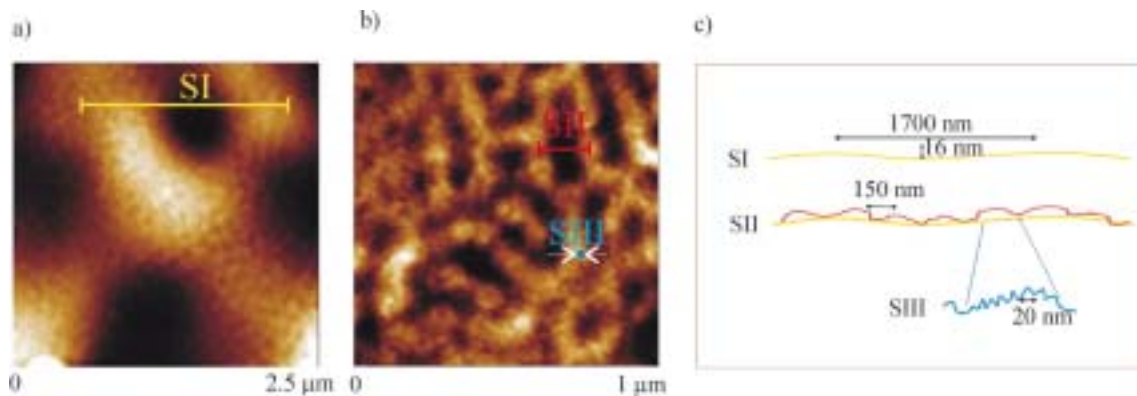


Fig. 6. AFM images of sample A5, recorded using the contact mode and presented in different scales: scale SI — a drop-like structure is visible (a), scales SII and SIII, revealing smaller surface fragments (b), and the surface features drawn schematically in the three scales (c)

different magnifications in the tapping mode, in which the cantilever was driven to oscillate up and down. As it is seen, the scratches are present on the surface of sample A0 (non-irradiated, Fig. 5a) while they are already absent in case of sample A3 (Fig. 5b). The PC surface becomes highly homogeneous and slightly rough. For a higher number of the laser pulses (sample A5, Fig. 5c), a surface of the drop-like structure is formed.

When analyzing the results, one has to keep in mind that the images shown in Figs. 4 and 5 cannot directly be compared because they represent surface areas significantly differing in size and, thus, demonstrating different geometrical structures (see the image edge sizes).

Figures 6a–c show the features of the surface geometrical structure of sample A5, presented in three various scales. In scale SI (Fig. 6a), the drop-like structure is clearly seen, the roughness average ( $R_a$ ), associated with the roughness profile height (PN-EN ISO 4287:1999), being *ca.* 16 nm. The drop-like structure is seen also in scale SII while the elements observed in scale SIII can be assigned to the fragments of PC macromolecules (Fig. 6b). The surface features drawn schematically in the three scales are illustrated in Fig. 6c for comparison.

One can suppose that thermal energy generated by both the laser radiation and the photochemical changes in PC is the main reason of formation of a new surface geometrical structure: this energy causes plasticization of the SL of polycarbonate the macromolecules of which can move to achieve a new thermodynamic equilibrium. The new surface (Fig. 7a) resembles the one that forms as a result of placing a liquid on a solid the SFE of which is smaller than SFE of the liquid (Fig. 7b).

The AFM images of surfaces of samples BX indicate that, due to ablation, their roughness increases and surface geometrical structures become different. The values of  $R_a$  for samples B0, B1, B3, and B4 are 8.2, 8.4, 71.4, and 128.1 nm, respectively. Two exemplary AFM images are shown in Figures 8a, b for sample B5. The laser irradiation causes also the changes in the colors of samples B1–B5, being probably the effects of intense photo-degradation of polycarbonate. The latter process may

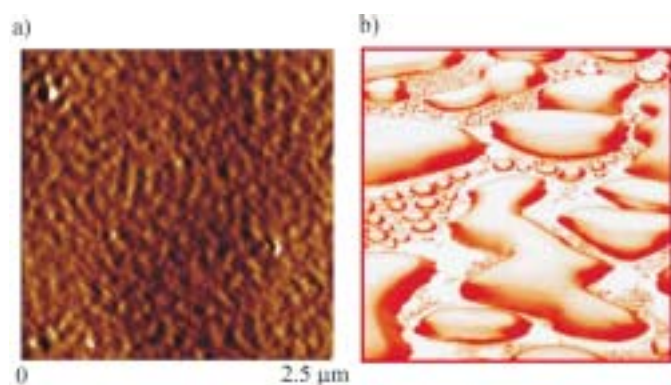


Fig. 7. Surfaces of a drop-like structure: an AFM image of sample A5, recorded using the contact mode method (a) and a digital image of a liquid on a glass surface (b) (see text)

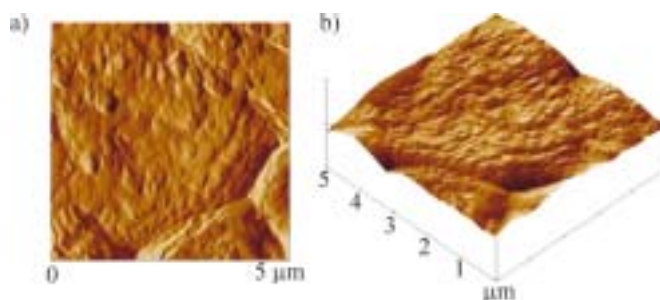


Fig. 8. AFM images of sample B5, recorded using the 2-D (a) and 3-D (b) techniques



Fig. 9. Optical microscopic image of sample B5, from which a surface layer fragment was removed by gentle rubbing (a light bar)

result in formation of graphite that is loosely bound to the material bulk and easily removable by gentle rubbing (Fig. 9).

### Wettability and surface free energy

Wettability of the individual samples was determined by the contact angle measurements performed 24 h after the sample irradiation. The contact angles of water ( $\Theta_W$ ) and diiodomethane ( $\Theta_D$ ) as functions of the number ( $N$ ) of the laser pulses are shown in Fig. 10a and Fig. 10b, respectively, for samples AX. As it is seen, both contact angles constantly decrease with the rising pulse number and are included in the ranges of  $91 \geq \Theta_W \geq 67$  and  $43 \geq \Theta_D \geq 33$  (so, the variation range of  $\Theta_W$  is *ca.* twice as much as that of  $\Theta_D$ ).

The dependence of  $\Theta_W$  on  $N$  for samples BX is plotted in Fig. 11, while Fig. 12 shows an image of a water droplet resting on the surface of sample B5 (the contact angle is *ca.*  $150^\circ$ ). That image was recorded with a camera coupled to a goniometer. Such a large contact angle indicates that the SL of polycarbonate gained a strongly hydrophobic nature. In case of diiodomethane, sample B5 is totally wettable ( $\Theta_D = 0$ ). That behavior may result from an enhancement of the dispersion interactions (*i.e.*, London forces, being the short-range van der Waals forces) among the macromolecules of PC and molecules of diiodomethane. This, in turn, is an effect of an increase in the sample roughness upon the laser irradiation and, thus, of enlargement of the area of contact between the

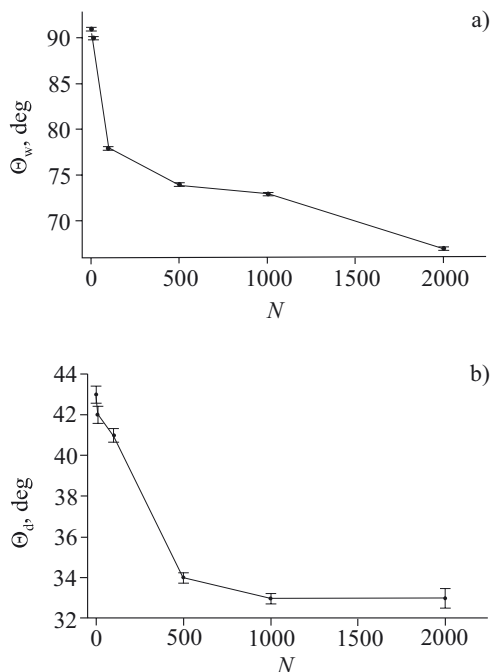


Fig. 10. Water contact angle ( $\Theta_W$ ) (a) and diiodomethane contact angle ( $\Theta_D$ ) (b) as functions of the number ( $N$ ) of laser pulses for samples AX

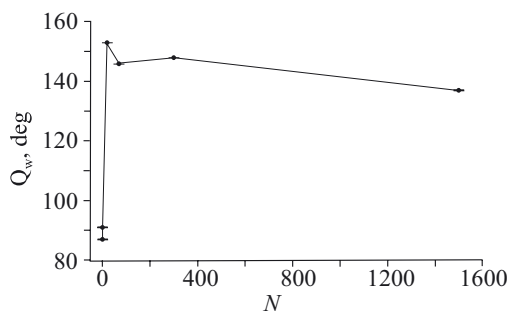


Fig. 11. Water contact angle ( $\Theta_W$ ) versus the number ( $N$ ) of laser pulses for samples BX

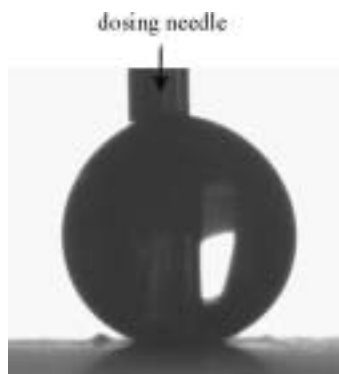


Fig. 12. Water droplet resting on the surface of sample B5 ( $\Theta_W \approx 150^\circ$ )

polymer and the test liquid. The results of  $\Theta_W$  and  $\Theta_D$  measurements indicate that SL of sample B5 contains mostly graphite, being ultra-hydrophobic and wettable with diiodomethane.

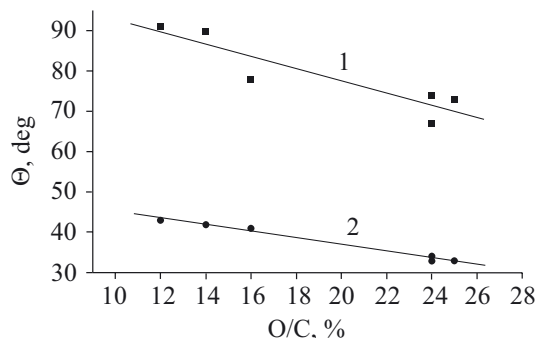


Fig. 13. Contact angles of water (1) and diiodomethane (2) as functions of the extent of oxidation ( $O/C$ ) of SL of samples AX

The wettability of PC depends on the elemental composition of its SL. Introduction of oxygen atoms into the polymer structure enhances polarity of the latter. The values of  $\Theta_W$  and  $\Theta_D$  were plotted versus an extent of oxidation (samples AX, Fig. 13) and the data were approximated with straight lines using the linear regression method. Clearly, the linear approximations fit well the experimental data.

The values of  $\Theta_W$  and  $\Theta_D$  were used to calculate the surface free energy. The total values and the polar and disperse components are plotted in Fig. 14 as functions of the number of the laser pulses used to irradiate the individual AX samples. It results from the figure that

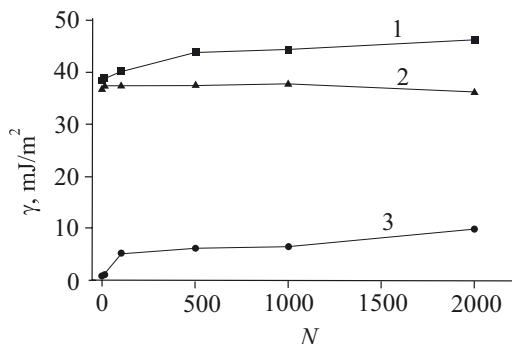


Fig. 14. Surface free energy ( $\gamma$ ) versus the number ( $N$ ) of laser pulses for samples AX: 1 — total SFE, 2 — dispersive component, 3 — polar component

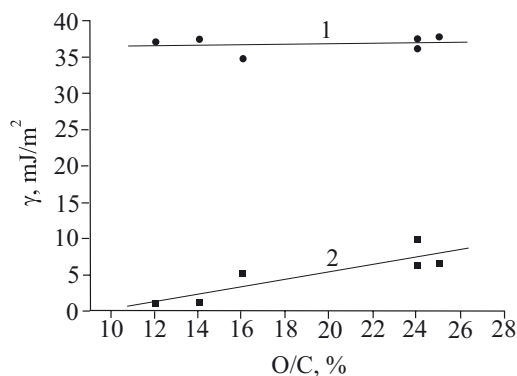


Fig. 15. Dispersive (1) and polar (2) components of SFE as functions of the extent of oxidation ( $O/C$ ) of SL of samples AX

SFE increases monotonically with the pulse number essentially due to the polar component (curve 3). When both SFE components are plotted *versus* the extent of oxidation, the data approximate to straight lines (samples AX, Fig. 15). The drawing indicates that the polar component (curve 2) slightly increases linearly with the rising O/C while the disperse component remains rather constant.

#### SUMMARY

The nature of physicochemical changes occurring in the surface layer of polycarbonate upon the laser radiation depends mostly on the radiation wavelength, unit energy of a laser pulse, and number of the laser pulses. Thus, these physicochemical changes are affected by the laser beam intensity and the total laser energy absorbed in the surface layer. When the unit energy of a laser pulse is below the ablation threshold for PC, the extent of oxidation of SL, surface roughness, surface free energy, and wettability of the modified polymer increase with the number of the pulses. This way, the adhesion properties of polycarbonate improve.

The quantitative changes in the extent of oxidation of SL, occurring mainly when the unit energy of a laser pulse is below the mentioned ablation threshold of the polymer, can be expressed by an exponential function including the number of the laser pulses as an independent variable. During the oxidation process, polar functional groups of different chemical compositions are formed.

Plasticization of polycarbonate due to generation and diffusion of heat as well as photochemical processes occurring in SL are the main factors that affect the changes in surface geometrical structure of the polymer. The changes result in a formation of so-called drop-like surface.

The larger SL extent of oxidation — the smaller contact angle and the larger surface free energy of PC. The polar component of SFE rises approximately linearly with O/C value while the disperse component remains roughly constant. The water contact angle increases with the number of the laser pulses of the unit energy above the ablation threshold while diiodomethane contact angle decreases. At the same time, surface roughness of PC enhances and SL is subjected to changes significantly different from those that occur upon irradiation with the laser pulses of the unit energy below the ablation threshold.

The results of the present work are important also for evaluation of the functional quality of the modified polymers. They suggest that for modification of the adhesion properties of polycarbonate the laser radiation wavelength below 308 nm should be used. This can be reached with ArF excimer laser, suitable for the processes mentioned. To achieve an essential improvement of

the adhesion properties, including enhancement of hydrophilicity of SL of polycarbonate, the laser pulses of the unit energy below the ablation threshold should be used. Irradiation with the pulses of the unit energy above this value would change the surface properties to strongly hydrophobic. However, the surface modified this way would become little resistant to abrasion.

#### REFERENCES

- Garbassi F., Morra M., Ochiello E.: "Polymer Surfaces. From Physics to Technology", Wiley & Sons, Chichester 1998, pp. 3—48.
- Żenkiewicz M.: "Adhesion and Surface Modification of Polymer Materials", WNT, Warsaw 2000, pp. 25—70, (in Polish).
- Kray D., Fell A., Hopman S., Mayer K., Willke G. P., Glunz S. W.: *Appl. Phys. A*, 2008, **93**, 99.
- Elaboudi I., Lazare S., Belin C., Talaga D., Labrugère C.: *Appl. Phys. A*, 2008, **92**, 743.
- Hwang D. J., Misra N., Grigoropoulos C. P., Minor A. M., Mao S. S.: *Appl. Phys. A*, 2008, **91**, 219.
- Fardel R., Nagel M., Lippert T., Nuesch F., Wokaun A., Luk'yanchuk B. S.: *Appl. Phys. A* 2008, **90**, 661.
- Bachmann F. G.: *Appl. Surf. Sci.* 1990, **46**, 254.
- Man H. C., Li M., Yue T. M.: *Int. J. Adhesion Adhesives* 1998, **18**, 151.
- "Adhesion. Current Research and Applications" (Ed. Possart W.): Wiley-VCH, Weinheim 2005, p. 305.
- Ardelean H., Petit S., Laurens P., Marcus P., Arefi-Khonsari F.: *Appl. Surf. Sci.* 2005, **243**, 304.
- Zeng J., Netravali A. N.: *J. Adhesion Sci. Technol.* 2006, **20**, 387.
- Yip J., Chan K., Sin K. M., Lau K. S.: *Appl. Surf. Sci.* 2003, **205**, 151.
- Beauvois S., Renaut D., Lazzaroni R., Laude L. D., Bredas J. L.: *Appl. Surf. Sci.* 1997, **109/110**, 218.
- Lippert T., Dickinson J. T.: *Chem. Rev.* 2003, **103**, 453.
- Oliveira V., Vilar R.: *Appl. Phys. A* 2008, **92**, 957.
- Pokorná D., Šubrt J., Galiková A., Pola J.: *Polym. Degrad. Stab.* 2007, **92**, 352.
- Khan F., Kwek D., Kronfli E., Ahmad S. R.: *Polym. Degrad. Stab.* 2007, **92**, 1640.
- Hitchcock L. M., Kim G-S., Peck G., Rothe E. W.: *Quantita Spectr. Radiat. Transf.* 1990, **44**, 373.
- Lazare S., Granier V.: *J. Appl. Phys.* 1988, **63**, 2110.
- "High Resolution XPS of Organic Polymers — The Scienta ESCA 300 Database" (Eds. Beamson D., Briggs D.), Wiley & Sons, Chichester 1992, p.152.
- "Practical Surface Analysis" (Eds. Briggs D., Seach M. P.), Wiley & Sons, Chichester 1998, pp.437—483.
- "Surface Analysis. The principal Techniques" (Ed. Vickerman J. C.), Wiley & Sons, Chichester 1997, pp.43—98.
- Georgiou S.: *Adv. Polym. Sci.* 2004, **168**, 1.

Received 26 VIII 2008.